

Macro-Micro Modeling Analysis of Melting and Re-solidification of thin Si Films by Excimer Laser Annealing

Long-Sun Chao^{1,a} and Chien-Hung Chang^{1,2,b}

¹Department of Engineering Science, National Cheng Kung University; 1 Ta-Hsueh Road, Tainan Taiwan, 701, R.O.C.

²Department of Mechanical Engineering Air Force Institute of Technology GangShan 820, Taiwan R.O.C.

^alschao@mail.ncku.edu.tw, ^bbag@hflow.es.ncku.edu.tw

Keywords: Macro-Micro Modeling, Nucleation, Poly-Si Thin Film, Laser Annealing Technology,

Abstract. In this work, an macro-micro model has been developed for the melting and resolidification of thin Si films induced by excimer-laser annealing. The macro-micro model, considering the formation of microstructures: nucleation and growth, can obtain the better results than macro-models. Except temperature distributions, the macro-micro models can offer more information about solidification process, such as undercooling, grain size, grain density etc. These data could help to predict the physical properties of materials. In this study, the finite difference method is utilized to solve the heat transfer problem. The specific heat/enthalpy method and the source term scheme are employed to handle the absorbed and released latent heat. The algorithm that allows for nucleation is based on classical nucleation theory. Accordingly, the model enables the prediction of grain size, as well as the calculation of other critical responses of the a-Si film, such as undercooling. From the computational results, it can be found that when the laser fluence is higher, the cooling rate after laser irradiation is lower, the maximum undercooling is smaller and the grain size is larger or the grain density is lower. The average grain sizes, obtained from the simulation results of the proposed model, agree fairly well with those from the experimental data reported in the literature. It can also be found that the reflectivity of the surface gives a good way to observe the phase changes and the melting duration.

Introduction

Recently, the excimer laser annealing (ELA) method is applied to the fabrication of the high performance thin film transistors (TFTs) of poly-crystalline silicon for active-matrix liquid crystal display [1]. The laser-crystallized poly-Si is also used in producing thin-film solar cells [2]. Accordingly, making poly-Si thin films on glass substrate has become an important fabricated process. From the researches of the laser processing of poly-Si thin films, it reveals that the crystal growth of poly-Si films strongly depends on the absorbed energy from the incident laser pulse. This indicates that the solidification process of poly-Si films is influenced by the transient temperature distributions in the Si film [3]. The control of surface temperature during the processing of a pulsed laser is of critical importance [4]. However, the temperature distributions of Si thin films are difficult to measure directly. Many labs have been trying to develop more accurate methods to find out the temperature distributions. Consequently, it is helpful and significant to make theoretical analyses on the temperature fields of the Si films irradiated by pulsed laser techniques.

Due to its technological importance, it is attractive to simulate the laser crystallization process in order to understand the effects of various process variables and optimize the conditions leading to a desirable microstructure. Many researches use macro-models to deal with the phase change in excimer-laser annealing that is determined by temperature only[5-7]. However, macro-models exclude phenomena, such as nucleation and undercooling, which are characteristically seen in ELA.

In this paper, we have developed a macro-micro model that takes into account the said phenomena. The macro-micro model, considering the formation of microstructures: nucleation and growth, can obtain the better results than macro-models. Except temperature distributions, the macro-micro models can offer more information about solidification process, such as undercooling,

grain size, grain density directly. An implicit finite difference method is used to handle the re-solidification process. The intensity is considered a constant. A Gaussian profile of laser pulse is employed [8].

Theoretical Analysis

Governing equation. D

the temperatures in the a-Si film. The incident laser pulse is defined by the trapezoid profile of laser intensity, defined by the following equation, using the appropriate numerical method are described.

An a-Si film of 5 μm thickness is irradiated by an excimer laser of 248 nm wavelength.

The laser pulse has a trapezoid profile of laser intensity, defined by the following equation, using the appropriate numerical method are described.

The laser pulse has a trapezoid profile of laser intensity, defined by the following equation, using the appropriate numerical method are described.

The laser pulse has a trapezoid profile of laser intensity, defined by the following equation, using the appropriate numerical method are described.

where ρ is density and k is thermal conductivity.

the radiation energy of the film.

The initial and boundary conditions are as follows:

(1) Initial condition

Before heating the workpiece, the initial temperature is 300K.

(2) Boundary condition

The boundary condition is the same as the initial condition.

and radiation.

where n is the normal direction of the boundary.

the environment temperature is 300K.

set to be 300K and ε is 0.01.

(ii) The boundary condition is the same as the initial condition.

Heat source term. Base

Q = I₀αe⁻^{az},

I₀ = { I₀(1 - R_c) heat in

0 the other

size, grain density etc. These data can help to predict the mechanical properties of materials directly. An implicit finite difference method is set up to solve the heat conduction equation whose thermal properties are function of temperature and the specific heat/enthalpy and source term methods are used to handle the release and absorption of latent heat. The spatial distribution of laser power intensity is considered as a trapezoidal shape while a time-dependent profile resembling the actual laser pulse is employed [8]. The computing results are compared with the experimental ones reported in literature.

Theoretical Analysis and Numerical Method

Governing equation. During the annealing process of excimer laser, it is quite difficult to measure the temperatures in the a-Si thin film. However, it is feasible to use a mathematical model to study the problem. The incident laser energy to the silicon surface is partly absorbed and partly reflected, relying on the reflectivity of the surface. Some of the absorbed energy is lost due to the convection and radiation heat transfers from the surface into the surrounding, while the rest is conducted throughout the silicon film and glass substrate. The absorbed radiation energy can be regarded as the heat source in the film or substrate. Heating and cooling periods can be resolved by solving numerically the heat equation, using the appropriate optical and thermal parameters. The mathematical models and numerical method are described as follows.

An a-Si film of 500Å in thickness on glass substrate is melted by the irradiation of a KrF excimer laser of 248 nm in wavelength and is cooled down to form a poly-Si film after irradiation. A trapezoid profile of laser intensity [8] is used in the numerical computation and the pulse duration is 25 ns, defined by the full width at half maximum (FWHM). The two-dimensional nonlinear heat diffusion equation with temperature-dependent thermal properties is given by:

$$\rho C_p^{\text{eff}} \frac{\partial T}{\partial t} = \frac{\partial}{\partial x} (k \frac{\partial T}{\partial x}) + \frac{\partial}{\partial y} (k \frac{\partial T}{\partial y}) + Q + \rho L \frac{\partial f_s}{\partial t}, \quad (1)$$

where ρ is density and k is thermal conductivity. Q is the heat source term, which is used to deal with the radiation energy of laser. C_p^{eff} is the effective specific heat. L is latent heat and f_s is the local volume fraction of solid.

The initial and boundary conditions of the model are

(i) Initial condition

Before heating the work piece, its temperature can be adjusted as desired. Accordingly, it can be room temperature, or larger or smaller than room temperature.

(2) Boundary condition

(i) The boundary condition from upper surface is that the heat is lost by a combination of convection and radiation.

$$-k \frac{\partial T}{\partial n} = h(T - T_{\infty}) + \varepsilon k_B (T^4 - T_{\infty}^4), \quad (2)$$

where n is the normal direction of boundary, h is the coefficient of convection heat transfer, T_{∞} is the environment temperature, ε is emissivity and k_B is the Stefan-Boltzmann constant. In this study, T_{∞} is set to be 300K and ε is 0.22 [9].

(ii) The boundary condition of the bottom surface can be heat-insulated or a fixed temperature, which is the same as the initial temperature.

Heat source term. Based on the Beer's law, the source term Q in Eq. 1 can be written as [10]

$$Q = I_0 \alpha e^{-\alpha z}, \quad (3)$$

$$I_0 = \begin{cases} I_i (1 - R_e) & \text{heating zone} \\ 0 & \text{the other place} \end{cases} \quad (4)$$

where I_t is the temporal distribution of the laser power per unit area, α is absorption coefficient, R_s is reflectivity. The magnitude of reflectivity would directly affect the absorptive energy of work piece from laser. Hatano et al. [9, 11] use an optical method to measure the reflectivity of the a-Si thin film. The reflectivity is obviously affected by surface temperature of silicon film, especially when the a-Si film is in the liquid state.

Latent heat and formation of microstructures. Macro-micro models differ from macro ones in the way of handling the latent heat. Before solidification, there is no difference between them. The enthalpy/specific heat method [12] is utilized to handle the latent heat during the melting process. It is the combined scheme of the enthalpy and the specific heat methods and has the advantages of these two methods, accuracy and fast convergence. The relationship among temperature, effective specific heat and enthalpy can be written as

$$Cp^{\text{eff}} = (e^{n+1} - e^n) / (T^{n+1} - T^n), \quad (5)$$

where e is enthalpy and Cp^{eff} is effective specific heat. Once the temperature is lower than the melting point, the source term [13] is used instead to deal with the latent heat and the calculation of local volume fraction of solid, f_s , is needed.

For the macro-micro models, since grains are assumed to be spherical, the local volume fraction of solid, f_s , can be given by

$$f_s(t) = N(t) \left[(4/3) \pi R^3(t) \right] \quad (6)$$

where $N(t)$ is grain number per unit volume and $R(t)$ is grain radius.

In the nucleation step, according to classical nucleation theory (CNT), the model accounts for nucleation that occurs in the bulk liquid (homogeneous) as well as on a accelerative surface such as the Si/glass interface (heterogeneous). From CNT, the homogeneous and heterogeneous rates of nucleation are given by Eqs.(7) and (8), respectively.

$$I_v(T_{i,i}) = I_{0v} \exp \left\{ -16\pi\sigma^3 / \left[3k_B T_{i,i} \Delta G_{ls}(T_{i,i})^2 \right] \right\} \quad (7)$$

$$I_a(T_{i,i}) = I_{0a} \exp \left\{ -16\pi\sigma^3 \cdot f(\theta) / \left[3k_B T_{i,i} \Delta G_{ls}(T_{i,i})^2 \right] \right\} \quad (8)$$

where k_B is Boltzmann's constant, I_{0v} and I_{0a} are kinetic prefactors, σ is surface energy, and $\Delta G_{ls}(T_i)$ is the difference in Gibbs free energy between liquid and solid phases. The heterogeneous rate includes the correction factor $f(\theta) = [2-3\cos(\theta)+\cos^3(\theta)]/4$. When $\partial T/\partial t > 0$ (i.e., the recalescence occurs), $dN = 0$. This is the end point of nucleation step.

In the growth step, the interface response function is used. The growth rate V is assumed to be

$$V = \mu \cdot \Delta T \quad (9)$$

where μ is a proportionality constant, whereas previous studies have placed the value of this constant in the range of 6.7–7.2 $\text{cm s}^{-1}\text{K}^{-1}$ [14]. ΔT is the undercooling which is equal to the difference of T_i and T_f . T_f is the melting temperature. The expression of R can be obtained by integrating Eq. (9).

$$R = r_0 + \int \mu [T_f - T(t)] dt \quad (10)$$

where r_0 is the critical radius.

The two-step Close-Pack model [15] is applied for the impingement step. The f_s expression can be written as

$$df_s/dt = \phi \cdot 4\pi R^2(t) \cdot N(t) \cdot dR/dt \quad (11)$$

where

$$\phi = \begin{cases} 1 & T < T_f \\ -10.32 \log_{10}(f_s) & T \geq T_f \end{cases}$$

Numerical method

Since the finite difference method is used to solve these equations. Computation is carried out in the variation zone of temperature and time. Because the laser pulse is un-uniform, the un-uniform heat is considered.

Results and discussion

In order to measure the temperature history of a silicon film melt by a pulsed excimer laser, Hatano et al. [9] have achieved the estimation of the transient temperature of the film melt. The simulation provides the temperature history of the film melt. At about 200 nm, it is the end point of the nucleation step. This is in contrast to the homogeneous nucleation into a liquid droplet. The variations of the average grain sizes are very close to each other.

Fig. 1 Variations of front reflectivity

Another observation of the variation of front reflectivity of the silicon surface gives a result that the volume fraction of solid silicon is stable at 100% in nanoseconds, the reflectivity stays at 100% until the recalescence occurs, and the growth stage follows.

In general, it is the case that the higher cooling rate leads to a

sorption coefficient, R_s ,
ive energy of work piece
ivity of the a-Si thin film
especially when the a-Si

from macro ones in the
ence between them. The
the melting process. It is
s the advantages of these
perature, effective specific

(5)

is lower than the melting
the calculation of local

he local volume fraction

(6)

the model accounts for
derative surface such as
heterogeneous rates of

(7)

(8)

ce energy, and $\Delta G_{\text{hs}}(T_d)$
The heterogeneous rate
(i.e., the recalescence

te V is assumed to be

(9)

ie value of this constant
l to the difference of T_d
integrating Eq. (9).

(10)

The f_s expression can

(11)

$$f_s = \begin{cases} -10.32 \log_{10}(f_s) & 1 \geq f_s \geq 0.8 \\ 1 & f_s < 0.8 \end{cases} \quad (12)$$

Numerical method. The governing equation was solved by using the finite difference method. Since the finite difference equations are nonlinear equations, the iterative method is used to solve these equations. Compared with glass substrate, the a-Si film is very thin as well as the primary variation zone of temperature. Accordingly, the unequal-spacing grid is used along the depth direction. Because the time between two laser shots is much larger than the duration time of a laser pulse, the un-uniform time step is utilized. The thermal properties used in this calculation are derived from Ref. 9, 16 and 17, in which the temperature dependence of the thermal conductivity and specific heat is considered.

Results and discussion

In order to measure the transient temperature and front reflectivity evolution when irradiated by a excimer laser, Hatano et al. [9, 11] used *in situ* nanosecond time-resolved optical diagnostics to achieve the estimations. The same experimental laser parameters are used in the calculation of transient temperature distribution and front reflectivity during the irradiation of the excimer laser. The simulation provides detailed information about the solidification process. Fig. 1 shows the temperature history on the Si surface at the beam center, which is seen to rise to about 1550 K as the film melts. At about 27 ns, the undercooling reaches to maximum value (i.e., the recalescence occurs) and it is the end point of nucleation with subsequent rise in temperature due to the released latent heat. This is in contrast to the macro-model (shown by the dashed line), which does not take undercooling and nucleation into account. Fig. 2 shows a comparison between the measured [9] and calculated variations of the average grain sizes versus laser fluences. In the figure, the computed average grain sizes are very close to the measured ones.

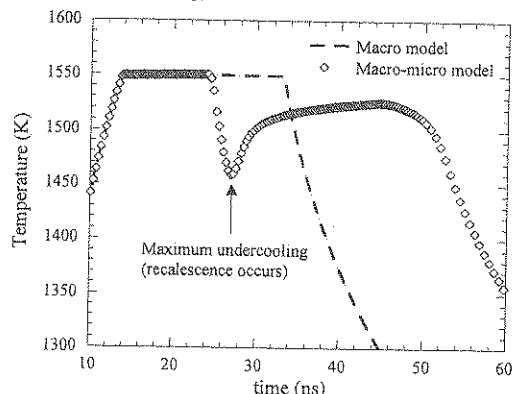


Fig. 1 Variation of computed surface temperature of the silicon film versus time

Another observational quantity is the temporal variation of front reflectivity. Fig. 3 shows that the variation of front reflectivities are consistent with the front temperatures. The reflectivity of the silicon surface give a good way to observe the phase change and the melting duration. The reflectivity of solid silicon is small, however, that of liquid silicon is large. In Fig. 3, in the first several nanoseconds, the reflectivity goes up to a value, which is the reflectivity of liquid silicon. The reflectivity stays at this value for a while, which is the duration time of liquid silicon. After the recalescence occurs, the reflectivity increases from a local minimum, which means it turns into the fully growth stage from the nucleation one.

In general, it is thought that the higher cooling rate (dT/dt) yields the larger grain density since the higher cooling rate leads to the greater undercooling, which causes the larger number of nuclei [18].

This is consistent with the computed results, as shown in Fig. 4, which illustrates the distributions of the maximum undercooling and grain sizes. From the figure, it can be found the grain sizes are strongly related to the undercooling. When the laser fluence is higher, the cooling rate after laser irradiation is lower, the maximum undercooling is smaller and the grain size is larger or the grain density is lower.

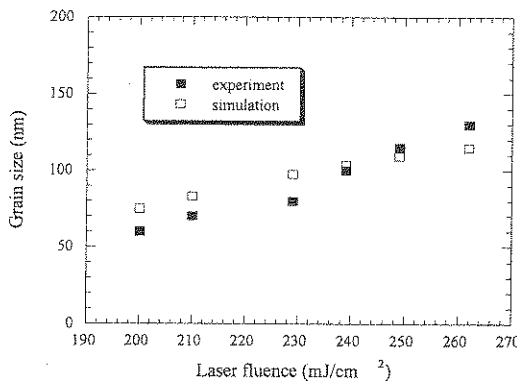


Fig. 2 Grain size versus laser fluence

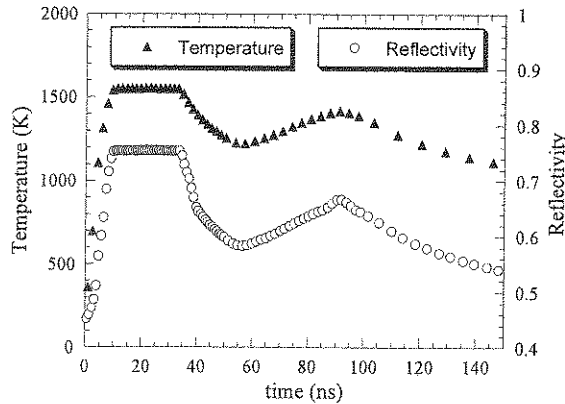


Fig. 3. Transient computed distributions of front reflectivity and temperature at the laser fluence of 262 mJ/cm^2 .

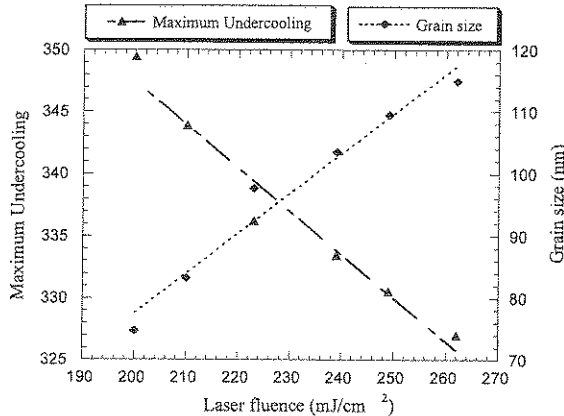


Fig. 4 Maximum undercooling and grain sizes versus laser fluences

Conclusions

To obtain good quality material, it needs to find the appropriate process parameters of laser. It is feasible and helpful to be used in this paper, an efficient technique of a poly-Si film, an important whose thermal properties and term scheme are used to be compared with the experimental results. It is found that when the laser fluence is lower, the maximum undercooling is higher and the average grain sizes, obtained from the experimental results, are smaller. The surface gives a good quality material. As mentioned above, the analysis and experimental results can be used to predict the quality of the material.

References

- [1] S.D. Brotherton, D.J. Sandercock, *Int. J. Heat Mass Transfer*, 40, (1997), p. 4086.
- [2] R.B. Bergmann, J. K. Strohmeier, *Int. J. Heat Mass Transfer*, 41, (1998), p. 587.
- [3] K. Shimizu, S. Imai, T. Kondo, *Int. J. Heat Mass Transfer*, 41, (1998), p. 2001.
- [4] S. Chen and C. P. Grigoropoulos, *Int. J. Heat Mass Transfer*, 41, (1998), p. 2011.
- [5] R. Wood and G. Geissler, *Int. J. Heat Mass Transfer*, 41, (1998), p. 2021.
- [6] J. Viatella, S. Lee, and C. P. Grigoropoulos, *Int. J. Heat Mass Transfer*, 41, (1998), p. 2031.
- [7] P. Baeri, S. Campisano, and C. P. Grigoropoulos, *Int. J. Heat Mass Transfer*, 41, (1998), p. 2041.
- [8] B. S. Yilbas: *Int. J. Heat Mass Transfer*, 41, (1998), p. 2051.
- [9] M. Hatano, S. Moon and C. P. Grigoropoulos, *Int. J. Heat Mass Transfer*, 41, (1998), p. 2059.
- [10] Michael F. Modest: *Radiation Heat Transfer*, McGraw-Hill, New York, 1993, p. 295.
- [11] C. P. Grigoropoulos, *Int. J. Heat Mass Transfer*, 41, (1998), p. 2069.
- [12] J. A. Dantzig: *International Heat Transfer Conference*, 1998, p. 1769.
- [13] V. R. Voller, and C. P. Grigoropoulos, *Int. J. Heat Mass Transfer*, 41, (1998), p. 2079.
- [14] A. K. Jena, and M. C. Cross, *Phase Transformations in Crystalline Solids*, Cliffs, N.J., 1992.
- [15] P. Alexandre, M. C. Cross, *Phase Transformations in Crystalline Solids*, Cliffs, N.J., 1992.
- [16] H. Kisdarjono, A. T. Yilbas, *Int. J. Heat Mass Transfer*, 41, (1998), p. 4374-4381.
- [17] H. Kuriyama, S. Kiyama, T. Osumi, S. Tsuda, S. Nakajima, *Int. J. Heat Mass Transfer*, 41, (1998), p. 2091.
- [18] W. Kurz, and D. A. Volman, *Laser Processing of Materials*, Birkhäuser, Berlin, 1991.
- [19] W. Kurz, and D. A. Volman, *Laser Processing of Materials*, Birkhäuser, Berlin, 1991.

rates the distributions of
and the grain sizes are
cooling rate after laser
size is larger or the grain

Conclusions

To obtain good qualities of poly-Si films fabricated by using the excimer laser crystallization method, it needs to find out the optimum working conditions. This needs to analyze the influences of process parameters of laser. The experimental approaches are very time-consuming and costly. It is feasible and helpful to build an appropriate mathematical model, which can be solved numerically. In this paper, an efficient two-dimensional macro-micro model is developed for the fabricating process of a poly-Si film, an implicit finite difference method is set up to solve the heat conduction equation whose thermal properties are function of temperature. The specific heat/enthalpy method and source term scheme are used to handle the release or absorption of latent heat. The computing results are compared with the experimental ones reported in literature. From the computational results, it can be found that when the laser fluence is higher, the cooling rate after laser irradiation is lower, the maximum undercooling is smaller and the grain size is larger or the grain density is lower. The average grain sizes, obtained from the simulation results of the proposed model, agree fairly well with those from the experimental data reported in the literature. It can also be found that the reflectivity of the surface gives a good way to observe the phase changes and the melting duration. From the results mentioned above, the analysis of the proposed macro-micro model combined with the corresponding experimental results can deeply study the problem of poly-Si film fabrication.

References

- [1] S.D. Brotherton, D.J. Mcculloch, J.P. Gowers, J.R. Ayres and M.J. Trainor: *J. Appl. Phys.* Vol. 82 (1997), p. 4086.
- [2] R.B. Bergmann, J. Kohler, R. Dassow, C. Zaczek and J.H. Werner: *Phys. Stat. Sol. (a)* Vol. 166 (1998), p. 587.
- [3] K. Shimizu, S. Imai, O. Sugiura and M. Matsumura: *Jpn. J. Appl. Phys.* Vol. 30 (1991), p. 2664.
- [4] S. Chen and C. P. Grigoropoulos: *Appl. Phys. Lett.* Vol. 71 (1997), p. 3191.
- [5] R. Wood and G. Geist, *Phys. Rev. B* Vol. 34, (1986), p. 2606.
- [6] J. Viatella, S. Lee, and R. Singh, *J. Electrochem. Soc.* Vol. 146, (1999), p. 4605.
- [7] P. Baeri, S. Campisano, G. Foti, and E. Rimini, *J. Appl. Phys.* Vol. 50, (1979), p. 788.
- [8] B. S. Yilbas: *Int. J. Heat Mass Transfer* Vol. 40 (1997), p. 1131.
- [9] M. Hatano, S. Moon and M. Lee: *Journal of Applied Physics* Vol. 87 (2000), p. 36.
- [10] Michael F. Modest: *Radiative Heat Transfer* (McGraw-Hill Book Company, 1993).
- [11] C. P. Grigoropoulos, S. Moon, M. Lee, M. Hatano and K. Suzuki: *Appl. Phys. A.* Vol. 69 (1999), p. 295.
- [12] J. A. Dantzig: *International Journal of Numerical Methods in Engineering* Vol. 28 (1989), p. 1769.
- [13] V. R Voller, and C. R. Swa, *Numerical Heat Transfer*, Vol. 19, (1991) p. 175-189.
- [14] A. K. Jena, and M. C. Chaturvedi, *Phase Transformation in Materials* (Prentice Hall, Englewood Cliffs, N.J., 1992).
- [15] P. Alexandre, M. Castro, and M. Rappaz, in: *Modeling of Casting, Welding and Advanced Solidification Processes V*, The Minerals, Metals and Materials Society, Warrendale, PA, U.S.A (1991).
- [16] H. Kisdarjono, A. T. Voutsas, and R. Solanki, *Journal of Applied Physics*, Vol. 94, (2003) p. 4374-4381.
- [17] H. Kuriyama, S. Kiyama, S. Noguchi, T. Kuwahara, S. Ishida, T. Nohda, K. Sano, H. Kawata, M. Osumi, S. Tsuda, S. Nakano and Y. Kuwano: *Jpn. J. Appl. Phys.* Vol. 30 (1991), p. 3700.
- [18] W. Kurz, and D. J. Fisher: *Fundamentals of Solidification*, (Trans Tech Publications, Aedermannsdorf, Switzerland, 1989).